Correcting the Chromatic Aberration in Barrel Distortion of Endoscopic Images

Y. M. Harry Ng
Department of Automation and Computer-Aided Engineering
The Chinese University of Hong Kong
harry.ng@ieee.org

and

C. P. Kwong
Department of Automation and Computer-Aided Engineering
The Chinese University of Hong Kong
cpkwong@acae.cuhk.edu.hk

ABSTRACT

Modern endoscopes offer physicians a wide-angle field of view (FOV) for minimally invasive therapies. However, the high level of barrel distortion may prevent accurate perception of image. Fortunately, this kind of distortion may be corrected by digital image processing. In this paper we investigate the chromatic aberrations in the barrel distortion of endoscopic images. In the past, chromatic aberration in endoscopes is corrected by achromatic lenses or active lens control. In contrast, we take a computational approach by modifying the concept of image warping and the existing barrel distortion correction algorithm to tackle the chromatic aberration problem. In addition, an error function for the determination of the level of centroid coincidence is proposed. Simulation and experimental results confirm the effectiveness of our method.

Keywords: Barrel Distortion, Chromatic Aberration, Distortion Correction, Endoscopy, Centroid Estimation and Expansion Coefficients.

1. INTRODUCTION

Minimally Invasive Therapy is increasingly popular because of the use of natural or artificial orifices of the body for surgical operations, which minimizes the destruction of healthy tissues and organs. Electronic endoscopy employing miniature CCD cameras plays an important role in the diagnostic and therapeutic operations of Minimally Invasive Therapy. However, the high level of barrel distortion introduces nonlinear changes in the image: areas near the distortion center are compressed less and areas farther away from the center are compressed more. Because of this phenomenon, the outer areas of the image look significantly smaller than the actual size. Fortunately, this kind of distortion may be corrected by calculating the correction parameters based on least square estimation. Several researchers have proposed various mathematical models of image distortion and techniques to find the model parameters for distortion correction. For instance, Hideaki et al. [1] have derived a moment matrix from a set of image points and proposed to straighten distorted grid lines in the image based on the smallest characteristic root of this matrix. Asari et al. [2] have proposed a technique based on least squares estimation to find the coefficients of a correction polynomial, to which Helferty et al. [3] later provided an improved method. Specifically they proposed a technique which finds solutions in which all lines are parallel. Unlike previous approaches, both horizontal and vertical line fits are required to find the optimal distortion center and hence the overall solution. Nevertheless, the above methods concern only the geometric barrel distortion. In our case, we are interested in reducing the chromatic aberration in the barrel distortion of endoscopic images.

For the correction of chromatic aberration, an achromatic doublet consisting of two thin lenses that are separated or in contact so that its focal length is independent of wavelength is used [4][5]. Normally one lens is converging and the other is diverging, and they are often cemented together. As it is not possible to fully correct all aberrations, combining two or more lenses together for the correction is required. High-quality lenses used in cameras, microscopes, and other devices are compound lenses consisting of many simple lenses. A typical high-quality camera lens may contain six or more lenses. On the other hand, Willson et al. [6] proposed active lens control to correct the chromatic aberration. In the modern endoscope, compound achromatic lenses for correcting chromatic aberration are commonly used.

In this paper, we investigate the chromatic aberration in the barrel distortion of endoscope. J. Garcia et al. [7] have extracted three RGB color channels of an image for the measurement of the defocusing from the continuous light spectrum. Because of the depth of field, we assume the

images are focused already and the lateral chromatic aberration can be regarded as difference in magnification for different colors. Indeed, the chromatic correction can be performed either using a theoretical model of aberration formation or using experimentally measured aberration values. However, it is practically impossible to describe contributions of all parts of a particular optical system. Therefore, the use of experimentally measured aberration values is a much better choice. Thus, we take three monochromatic light samples, which are regarded as three RGB color channels. Then, we take a computational approach by modifying the concept of image warping [8] and the existing barrel distortion correction algorithm by Helferty et al. [3] to tackle the chromatic aberration problem. Once the correction polynomial coefficients are found, the correction of the chromatic aberration in barrel distortion of endoscopic images can be carried out. As the polynomial expansion coefficients are not changed with the distance from the object to the camera lens, the expansion coefficients obtained at a certain distance can be used to correct the image captured at any distance within the depth of field range [9]. In addition, an error function for the determination of the level of centroid coincidence is proposed. Finally, we use simulation and experimental results to confirm the effectiveness of our method.

2. THRORETICAL MODEL OF CORRECTION

There have been many studies on the computational correction of barrel distortion. In this paper, we mainly focus on the method proposed by Helferty et al. [3], of which the correction of the mapping from distortion space to correction space for black and white images is,

$$\rho = \sum_{n=1}^{N} a_n \rho'^n \quad , \quad \theta = \theta' \qquad (1)$$

where a_n is the set of correction expansion coefficients of an endoscope, ρ' and ρ are the radius from the distortion center to a point in the distortion space and the correction space, respectively, and θ' and θ are the angles of the point in the distortion space and the correction space, respectively. The basic experimental procedure, as suggested by Helferty et al., is to compute the correction expansion coefficients from an endoscopic video image of an image consisting of an equally spaced array of black dots on a white background. Once this correction is computed, it can be applied to live endoscopic video in real time.

An important property of visible light is its color, which is related to the wavelengths or frequencies of light. Visible light sensitive to human eyes falls in the wavelength range of about 400 nm to 750 nm. This is known as the visible spectrum and represents different

colors from violet to red. Light with wavelength shorter than 400 nm is called ultraviolet (UV), and light with wavelength greater than 750 nm is called infrared (IR). A prism separates white light into rainbow of colors. This happens because the index of refraction of a material depends on the wavelength. With reference to the concept of correcting chromatic aberration using image warping from Boult et al. [8], the geometric distortions must be computed and the red and green images must be fitted to a cubic spline. Since the light is a continuous spectrum, we can not deal only with three separate channels. In order to replace the achromatic lenses by computational correction, we need to take as many light samples as we can. In the meantime, we develop an error function which is used to determine how good the fitting of a cubic spline in the chromatic aberration in barrel distortion of endoscopic images is. We assume that the tested white light source only consists of three monochromatic light sources and they are belonged to the three color channels. Thus, the mappings from the distortion space to the correction space for the tested white light source are,

$$r_R = \sum_{n=1}^{N} a_{nR} r'^n_R \quad , \quad \theta_R = \theta'_R$$

$$r_G = \sum_{n=1}^{N} a_{nG} r'^n_G \quad , \quad \theta_G = \theta'_G$$

$$r_B = \sum_{n=1}^{N} a_{nB} r'^n_B \quad , \quad \theta_B = \theta'_B \qquad (2)$$

where a_{nR}, a_{nG} and a_{nB} are the set of correction expansion coefficients in red, green and blue color, respectively, and r' and r are the radii from the distortion center to the point in the distortion space and the correction space, respectively with its corresponding color. θ' and θ are the angles of the point in the distortion space and the correction space, respectively with its corresponding color. The goal of the processing is to calculate the coefficients of $a_{1R},...a_{nR}$, $a_{1G},...a_{nG}$, $a_{1B},...a_{nB}$.

Although we have found the coefficients for three colors, the corrected images may not be coincided with each other. In order to compensate the dispersion of the three colors, we make fine adjustments of the correction polynomial coefficients. Thus, an error function is now being proposed. As the green color centroid is located in the middle of red and blue color centorids, we choose the green color centroid and the green color correction polynomial coefficient as the desired control point. Then, we can finely adjust the correction polynomial coefficients by the following proposed method. First, we compute the distance of the farthest dot centroid in 45 degree from the center point of the image as,

$$D = \sqrt{(x^c)^2 + (y^c)^2} \qquad (3)$$

where D is the distance of the farthest dot centroid in 45 degree from the center point of the image, x^c is the value of the dot centroid in the x-direction and y^c is the value of the dot centroid in the y-direction. Secondly, the error function is,

$$E = |D - d| \qquad (4)$$

where D is the distance of the specific farthest dot centroid in 45 degree from the center point of the image, and d is the distance of the green farthest dot centroid in 45 degree from the center point of the image. Finally, we determine whether the value of the error function falls within the tolerance value ε. If the answer is yes, we accept the corresponding correction coefficients. Otherwise, we adjust the correction coefficients and compute the error function iteratively until the later is within the tolerance. The flow chart of the overall procedures for the fine adjustment of the correction polynomial coefficients is shown in Figure 1.
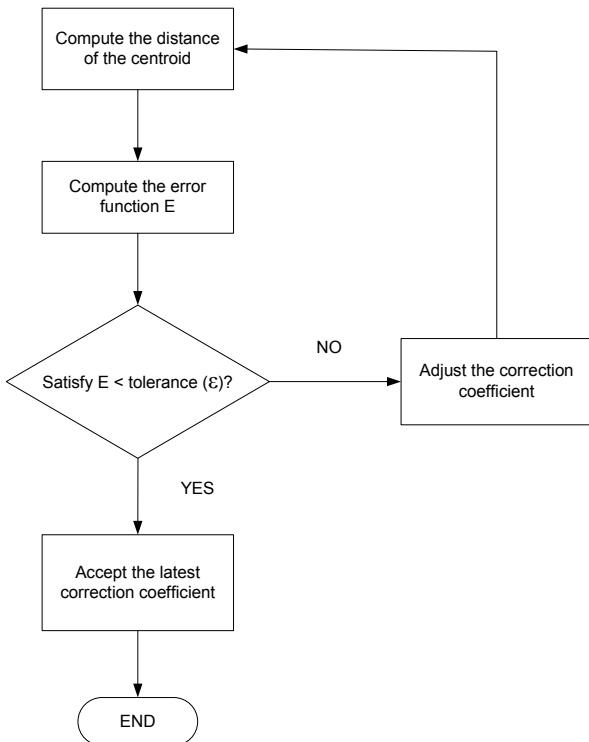

Figure 1. Flow chart of the overall procedure for the fine adjustment of the correction polynomial coefficients

For the centroid estimation, the centroid for each dot can be calculated as Eq. (5) and Eq. (6):

$$x_{ij}^c = \frac{1}{N} \sum_{n}^{N} x_{ijn} \qquad (5)$$

where x_{ij}^c is the value in the x-direction of the centroid of dot_ij (row i and column j), x_{ijn} is the value in the x-direction of the dot_ij elements and N is the number of the dot_ij elements in a pixel.

$$y_{ij}^c = \frac{1}{N} \sum_{n}^{N} y_{ijn} \qquad (6)$$

where y_{ij}^c is the value in the y-direction of the centroid of dot_ij (row i and column j), y_{ijn} is the value in the y-direction of the dot_ij elements and N is the number of the dot_ij elements in a pixel. Moreover, we can analyze the correction of barrel distortion by observing the area of the dots. The area for each dot can be calculated as,

$$A_{ij} = N \qquad (7)$$

where A_{ij} is the area of the dot_ij (row i and column j) and N is the number of the dot_ij elements in a pixel.

3. EXPERIMENTAL SETUP

In order to investigate the proposed method in noisy environment, we perform an experiment to capture images and make the corresponding calibration. Also, by experiment, we may compare simulation with the experimental results. This allows us to investigate the effectiveness of our method. The experimental setup of the optical platform for recording an image (white source grid pattern) is shown in Figure 2. It mainly consists of a camera, a supporting platform for the camera, a white source test grid pattern and a stage for the fixation of the test grid pattern.

Figure 2. Experimental setup of the optical platform for recording

The calibration dot pattern is a picture consisting of a square 7 x 7 array of white dots. Each dot is a 7mm x 7mm square. The distance between the dot centroids is 20mm. The dot pattern portion of the captured still image is 210 x 210 pixels. When capturing a test still image, we position the test dot pattern 360mm away from the WebCam lens. Distance of 360mm is a suitable distance since the dot pattern would fill the viewing area of the camera. The Web Cam we used is a Logitech QuickCam Express.

4. RESULTS

All of the simulations are performed with MATLAB 6.1. For the chromatic aberration in barrel distortion of white light source (the white light source grid pattern only contains three monochromatic light), the simulation aims to animate the endoscopic image captured by an endoscope with chromatic aberration. It is shown in Figure 3. The computer-corrected image is shown in Figure 4.
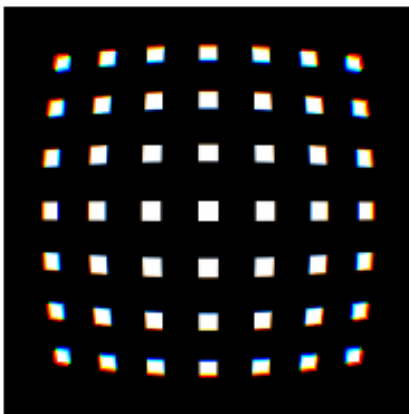

Figure 3. Simulation of chromatic aberration
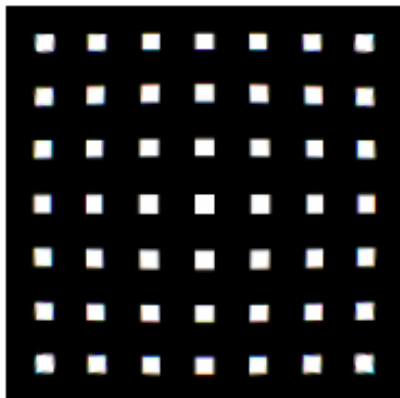in barrel distortion of white light source

Figure 4. Simulation of correction of chromatic aberration
in barrel distortion of white light source

We see that the distorted white source grid pattern is corrected in both the barrel distortion and the chromatic aberration. Also, we analyze the area of the dots in three colors with respect to the change in distance from the dots to the center of distortion. This can help us to determine the performance of the correction in barrel distortion for three colors. In addition, we also analyze the centroid of the dots in three colors with respect to the change in distance from the dots to the center of distortion. This can help us to determine the performance of the correction in chromatic aberration for three colors. The plot of area of dots versus distance from the center for simulated original, distorted and corrected images is shown in Figure 5. The plot of centorids of the dots versus distance from the center for simulated original, distorted and corrected images is shown in Figure 6.

From the middle plot of Figure 5, we see that the area of the third dot is significantly decreased. Also, the three colors are dispersed. This means that the image captured also undergoes chromatic aberration. Fortunately, after the correction we proposed, the area of the dot is retained and the dispersion of the three colors is reduced. It shows the effectiveness of our method for the correction of chromatic aberration in barrel distortion of images.
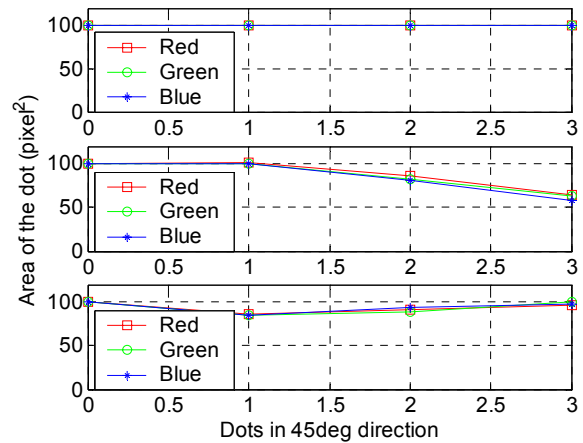

Figure 5. Plot of area of dots versus distance from the center for simulated original (top), distorted (middle) and corrected (bottom) image respectively.

From the middle plot of Figure 6, we see that the centroid distance from origin is reduced when comparing to the original image. Also, the image undergoes the dispersion of three colors. Thus, chromatic aberration is found. After the correction we proposed, the centroid distance form the origin is retained. The dispersion of three colors is reduced significantly.
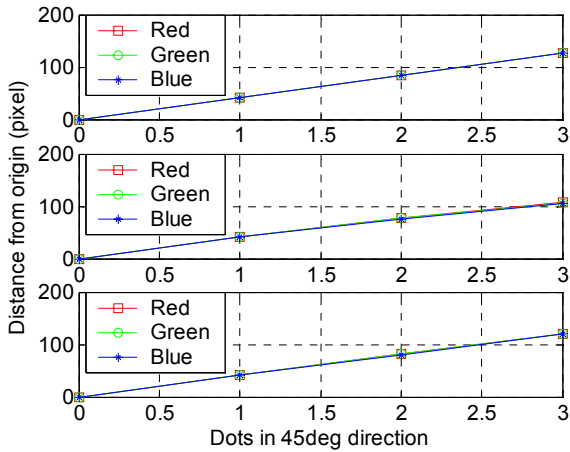
Figure 6. Plot of centorids of dots versus distance from
the center for simulated original (top), distorted (middle)
and corrected (bottom) image respectively.

The magnified view of plot of centroid of the third dot
versus distance from the center in corrected image of
Figure 6 is shown in Figure 7. We see that the dispersion
of three colors is minimized to less than 0.1 pixel. Thus,
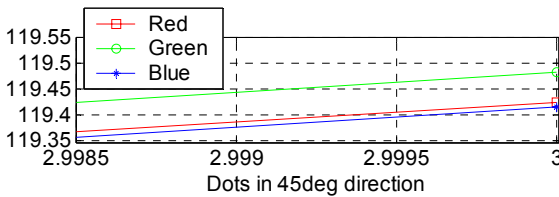the correction method we used is effective.

Figure 7. Magnified view of plot of centroid of the third
dot versus distance from the center
in corrected image of Figure 6.

In the experiment, we firstly captured the image by the
QuickCam Express from Logitech on a notebook
computer (1.6 GHz Pentium 4 and 256MB RAM) with
the Windows XP Home Edition Operating System. The
image and dot-pattern extraction were using the
QuickCam Express software package. Software for the
remaining off-line parameter calculation and display
processing was developed by using MATLAB 6.1 from
The MathWorks, Inc. Since it is not a real endoscope, it
does not undergo a great amount of barrel distortion. Also,
the chromatic aberration is not severe due to the existence
of the achromatic lenses system in the lenses originally.
In order to see the effects of correction clearly, we have
amplified the level of barrel distortion and chromatic
aberration of the extracted image. Though the
amplifications of both of the barrel distortion and
chromatic aberration are, the noisy environment is still
remained. In addition, if we can correct it even though it
is amplified, the original non-amplified image must be
corrected definitely. Then, we analyze the difference
between the simulation case and the experimental case

(with noisy environment). Thus, the feasibility of the
proposed method can be found. Figure 8 shows the
amplified extracted white light source (we define the
white light source grid pattern only contains three
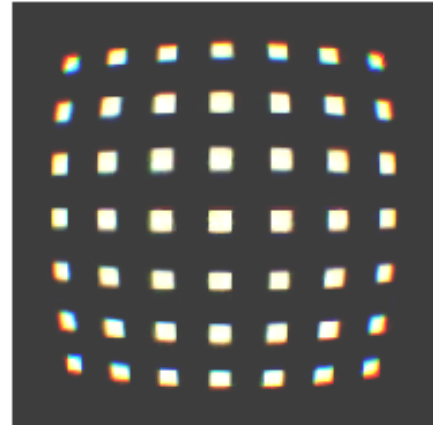monochromatic light) in the experiment.

Figure 8. Amplified extracted white light source
for the experiment

After obtaining the amplified image, we use our method
to correct both of the barrel distortion and chromatic
aberration in the amplified image. Fortunately, the result
is satisfied. Figure 9 shows the corrected image of
amplified extracted white light source for the experiment.
By observation of Figure 8 and 9, we can see that both of
the barrel distortion and chromatic aberration are
corrected experimentally. The magnified view of
amplified and corrected image is shown in Figure 10 and
11. We have chosen the dot at second row and sixth
column as reference point. From the Figure 10 and 11, we
can see that the chromatic aberration is corrected properly.
Although it still exists part of chromatic information, the
portion of chromatic image is reduced a lot. Also, the
white portion area of the dot is increased in the corrected
image. Thus, it shows the successful correction of
chromatic aberration in barrel distortion of image.
The tolerance value ε was set to 0.1 pixel in both of the
simulation and experiment. We can compare the corrected
image in simulation and corrected image in experiment in
Figure 4 and 9. For the ease of comparison, we can
compare the same dot in both of the correction in
simulation and correction in experimental case. Now, we
choose the dot at second row and sixth column as a
reference point. The magnified view of the dot in both of
the correction in experimental case and correction in
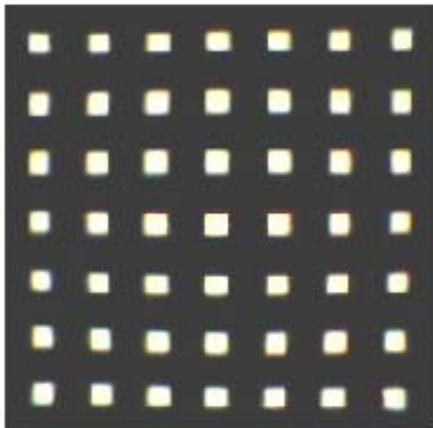simulation are shown in Figure 11 and 12, respectively.

Figure 9. Corrected image of amplified extracted white light source for the experiment
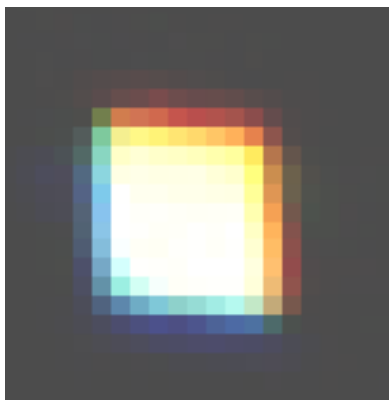

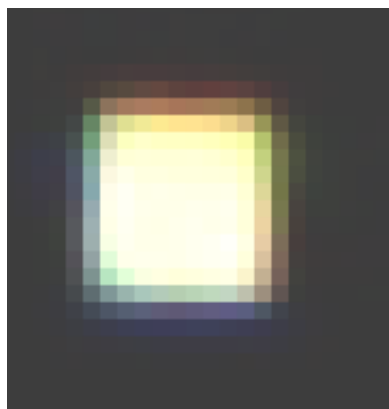Figure 10. Magnified view of the amplified image dot

Figure 11. Magnified view of the corrected image dot in experiment

simulation case. Nevertheless, the correction in experiment is acceptable even though it is not as good as the simulation case. When comparing the amplified image and corrected image in experiment which is shown in Figure 10 and 11, we can see that there is a great level of chromatic reduction. Thus, our method is effective.

Figure 12. Magnified view of the corrected image dot in simulation

The difference in performance may probably due to the fine adjustment of the proposed method which is determined by the level of centroid coincidence for three colors (we set the acceptable tolerance to 0.1 pixel). As the noise appeared, it may affect the determination of the actual centroid in the experimental case. Thus, the centroid we have may not be the exact centroid of the dot.

In order to investigate the effects in realistic images, we have used a real human videobronchoscopic image to test the effectiveness of our method. For the simulation of videobronchoscopic image without physical chromatic correction, we use the corrected image (video image of bifurcation) of Helferty et al. [3] as the input of undistorted image for the following simulations in Figure 13. As the actual light is a continuous spectrum, we only consider three different wavelength of light (red, green, blue). It can also be regarded as trichromat in nature. Indeed, many of achromatic lens system only concern two color light, such as red and blue. It is also called dichromat. Actually, by taking much more light samples, the result will be much more accurate. Since we are focusing on the feasibility of the algorithm for colored object, not the actual distorted image, the samples of light can be minimized to three. Once the actual chromatic correction is used, the quality of image will depends on the number of samples of light chosen. The simulation of barrel distortion and chromatic aberration of a human videobronchoscopic image (video image of bifurcation) without physical chromatic correction is shown in Figure 14.

From the Figure 12, we can see that the correction in simulation (without noise) is better than the experiment (with noise). The experimental image shows a slight rainbow color while the simulation image does not. Also, the area of white portion in simulation is larger than the area of the experiment for the same dot. Thus, we can conclude that the proposed method is operated better in
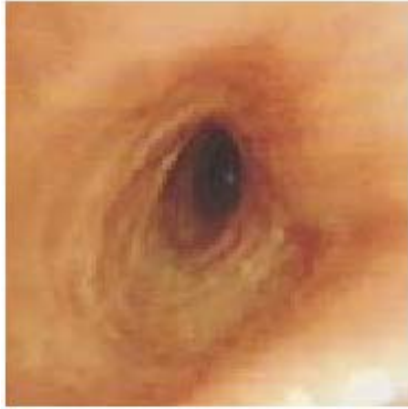
Figure 13. Corrected videobronchoscopoic image
(video image of bifurcation) taken from Helferty et al. [3]

Figure 14. Simulation of barrel distortion and chromatic
Aberration of the human videobronchoscopic image

The simulation of correction of the human videobronchoscopic image (video image of bifurcation) without physical chromatic correction is shown in Figure 15.

Figure 15. Simulation of correction of the human
Videobronchoscopic image

By comparing Figures 14 and 15, we see that the chromatic aberration can be largely corrected. Although there still exists part of chromatic information in the boundary, the proportion of chromatic aberration is reduced a lot.

5. CONCLUSIONS

In this paper, simulation and experimental result of correcting the chromatic aberration in barrel distortion of endoscopic images computationally are shown. Also, an error function for the determination of the level of centroid coincidence is proposed. We prove the effectiveness of our method by simulations and experimental results. Furthermore, the experimental results are compared with the simulation results.

7. REFERENCES

[1]   H. Hideaki, Y. Yagihashi, and Y. Miyake, "A new method for distortion correction of electronic endoscope images", **IEEE Trans. Med. Imaging**, Vol. 14, Sept. 1995, pp. 548-555.

[2]   K. V. Asari, S. Kumar, and D. Radhakrishnan, "A new approach for nonlinear distortion correction in endoscopic images based on least squares estimation", **IEEE Trans. Med. Imaging**, Vol. 18, Apr. 1999, pp. 345-354.

[3]   J. P. Helferty, C. Zhang, G. McLennan, and W. E. Higgins, "Videoendoscopic distortion correction and its application to virtual guidance of endoscopy", **IEEE Trans. Med. Imaging**, Vol. 20, July. 2001, pp. 605-617.

[4]   E. Hecht, **Optics**, Addison-Wesley Publishing Company, Reading, Mass., 1987.

[5]   V. N. Mahajan, **Optical Imaging and Aberration**, SPIE Optical Engineering Press, Washington, 1998.

[6]   R. G. Willson, and S. A. Shafer, "Active lens control for high precision computer imaging", **Proceedings of the 1991 IEEE International Conference on Robotics and Automation**, April 1991, pp. 2063-2070.

[7]   J. Garcia, J. M. Sanchez, X. Orriols, and X. Binefa, "Chromatic aberration and depth extraction", **Proceedings of the 2000 IEEE International Conference on Pattern Recognition**, Vol. 1, 2000, pp. 762-765.

[8]   T. E. Boult, and G. Wolberg, "Correcting chromatic aberrations using image warping", **Proceedings of the 1992 IEEE Computer Society Conference on Computer Vision and Pattern Recognition**, 1992, pp. 684-687.

[9]   H. Tian, T. Srikanthan, K. Vijayan Asari, and S. K. Lam, "Study on the effect of object to camera distance on polynomial expansion coefficients in barrel distortion correction," **Proceedings of the 2002 IEEE Southwest Symposium on Image Analysis and Interpretation**, 2002, pp. 255-259.